



## Detection of Blood Clots inside the Brain using Microwave Imaging

Farhana Parveen<sup>\*(1)</sup>, and Parveen Wahid<sup>(2)</sup>

(1) East West University, Dhaka-1212, Bangladesh

(2) University of Central Florida, Orlando, FL-32816, USA, Email: parveen.wahid@ucf.edu

### Abstract

In this paper, a microwave head imaging system is utilized for the detection of blood clots inside the brain. The imaging plane is divided into four quarters, and each quarter is scanned for imaging. A miniaturized wideband antipodal Vivaldi antenna is placed at nine different positions in front of each quarter of a numerical head model with blood clots for accumulation of reflected signals in a monostatic approach. The reflected signals are processed using delay-and-sum beamforming method to reconstruct an image of the head. Thus, four separate images are obtained by scanning through four quarters. Finally, a comparison of peak intensities obtained in the four images is made, where the observation of a higher intensity in a specific quarter could indicate the probable presence and approximate location of an anomaly, i.e., blood clot in that quarter.

### 1. Introduction

Microwave imaging can be considered as a promising alternative to the traditional brain imaging modalities, such as- MRI, CT scan etc. It allows for implementation using lightweight, portable, and inexpensive setups; involves a non-invasive process; and uses non-ionizing radiation. These factors override shortcomings of using this process, mainly precise image resolution. Commercialization of microwave head imaging needs further research and extensive experimentation.

Microwave head imaging entails antenna design and prototype development [1-3], the design of antenna array for brain monitoring [4, 5], numerical modeling of head [6], imaging system design [7, 8], processing and imaging algorithm development [9, 10], development of prototype head-imaging systems [11] etc.

In this work, a microwave head imaging system is incorporated using a quarter-head scanning based approach for the detection of blood clots inside the brain. In this approach, the entire imaging plane, i.e., a plane in the head is divided into four quarter portions, and a miniaturized wideband antipodal Vivaldi antenna is placed at nine different positions in front of each quarter to transmit electromagnetic wave and accumulate reflected signals from the head. An image of the head is

reconstructed focusing on each quarter by processing the reflected signals accumulated from that quarter. The peak intensities of four images obtained from four quarters are compared, and probable presence of an anomaly is suspected in a quarter which shows a higher intensity than that of the other quarters. Thus, the detection and approximate localization of an anomaly, i.e., blood clot, can be done using the microwave head imaging system.

### 2. Requirements and Challenges of Designing a Microwave Head Imaging System

For the design of an effective microwave head imaging system, there are several requirements that have to be met. The antennas need to (a) be small so that a portable setup can be devised and (b) provide wide frequency range of operation with directional radiation pattern. The small size can ensure accommodation of an array with large number of antennas in case of a multi-static setup, and the wide frequency band with directional pattern ensures proper penetration depth and image resolution, while focusing on a selective region inside the subject. As is known, low frequency signals can provide large penetration depth into the subject, whereas high frequency signals can provide high image resolution. Hence the operating frequency range used for the imaging should be carefully selected. The high permittivity of brain tissues causes very large signal attenuation at high frequencies, hence low frequencies are suitable for good penetration depth. However, as the image resolution is very poor at low frequencies, a wide frequency range (~ 1 – 4 GHz) is a better choice for proper resolution of the reconstructed image and sufficient penetration depth.

There are significant challenges associated with the antenna design to meet these conditions. Antenna dimensions get larger at lower resonating frequencies and obtaining a directional radiation pattern over a wideband of frequencies is difficult. Hence, the effective design of an antenna for use in a microwave head imaging system requires optimizing between some challenging trade-offs.

### 3. Antenna Design

A miniaturized wideband antipodal Vivaldi antenna is designed for use in a head imaging system. Details of the design are given in [12]. Figure 1 shows the antenna

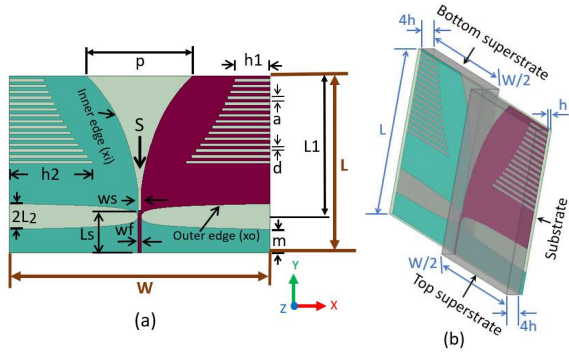
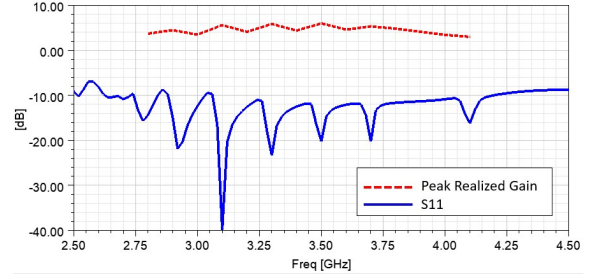


**Figure 1.** Miniaturized antipodal Vivaldi antenna- (a) top view, (b) isometric view; (parameters:  $L = 30.2$  mm,  $W = 44.4$  mm,  $a = d = 0.5$  mm,  $h1 = 6$  mm,  $h2 = 14.27$  mm,  $L1 = 24$  mm,  $L2 = 2.2$  mm,  $p = 18$  mm,  $wf = 0.5$  mm,  $m = 4$  mm,  $Ls = 7.2$  mm,  $ws = 0.5$  mm,  $h = 0.64$  mm). [12]

structure having length,  $L$  and width,  $W$  of 30.2 mm and 44.4 mm, respectively. The antenna is designed on Rogers RT/ duroid 6010 ( $\epsilon_r = 10.2$ , thickness,  $h = 0.64$  mm) as the substrate. To obtain a miniaturized antenna several techniques are adopted, including the use of corrugations, insertion of a slot near the feed, and addition of superstrates. Corrugations are introduced in both top and bottom layers of the antenna with 15 symmetrical slots on each layer. A slot ‘S’ is inserted near the feed region with width,  $ws = 0.5$  mm at a distance of  $Ls = 7.2$  mm away from the port. Two superstrates are added on both the top and bottom copper layers of the antenna, as shown in Figure 1b, each having dimensions of length,  $L = 30.2$  mm; width,  $W/2 = 22.2$  mm; and thickness,  $4h = 2.56$  mm. The same material (Rogers RT/ duroid 6010 with thickness 2.56 mm and  $\epsilon_r = 10.2$ ) as the substrate is used for the superstrates. The performance of the antenna is analyzed using ANSYS HFSS software, where the antenna is excited with a waveport. The reflection coefficient and peak realized gain of the antenna are shown in Figure 2. It can be seen that the antenna has  $S_{11} < -8$  dB from  $\sim 2.75$  GHz to 4.2 GHz with a bandwidth of  $\sim 1.45$  GHz. The antenna produces end-fire radiation within this frequency band. It can be seen from Figure 2 that, the antenna provides  $\sim 3 - 6$  dB peak realized gain within the  $S_{11} < -8$  dB frequency band.

#### 4. Imaging System Setup and Numerical Modeling

A quarter head scanning based approach is used here for the imaging. As shown in Figure 3a, the imaging region, i.e., a 2D plane in the head, is divided into four quarters and as shown in Figure 3b, the designed antenna is placed at nine positions, with the angular distance of  $10^\circ$  between two consecutive positions, in front of each of the quarters. At each position, in the monostatic approach, the reflection coefficient ( $S_{11}$ ) from 2.85 – 3.25 GHz with 0.1 GHz frequency step is recorded in the frequency domain. These reflected signals obtained from the nine positions at each quarter are processed for the reconstruction of an



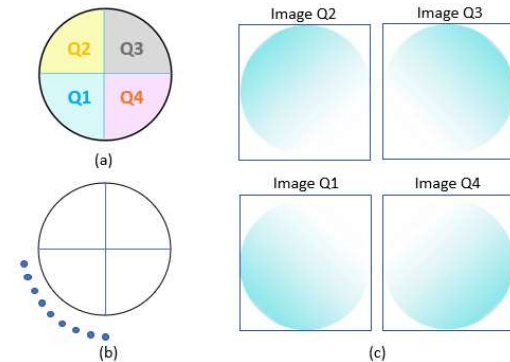
**Figure 2.** Reflection coefficient and peak realized gain of the antenna. [12]

image of the head, thus giving four images of the head by scanning through four quarters. Figure 3c shows the focusing region in the image of the head obtained by scanning through each quarter.

The head is modeled as a volumetric cross-section of a sphere with radius = 8 cm and thickness = 4 cm, with the brain being simulated as a homogeneous region with frequency non-dispersive material having effective relative permittivity,  $\epsilon_r = 40$ , dielectric loss tangent,  $\tan\delta = 0.27653$ , bulk conductivity,  $\sigma = 2.228$  S/m, mass density,  $\rho = 1042.67$  kg/m<sup>3</sup>. The blood clot is modeled as a coagulated blood region with  $\epsilon_r = 56.353$ ,  $\tan\delta = 0.32575$ ,  $\sigma = 3.6764$  S/m and  $\rho = 1080$  kg/m<sup>3</sup>. The antenna is placed at a distance of 4.5 cm away from the head model.

#### 5. Image Reconstruction

For the image reconstruction, first the reflected signals obtained from the nine positions in front of each quarter are converted from frequency domain to time domain. The time domain signals contain reflections from the background, air-head boundary, and clutter from inside the head, along with the target reflections arising from any anomaly, e.g., blood clot inside the brain. These artifacts in the obtained reflected signals are removed using the process mentioned in [12]. Signals prior to 1.2 ns are truncated to eliminate any residual air-skull



**Figure 3.** Microwave head imaging system: (a) division of a head plane into four quarters, (b) antenna positions in front of the first quarter, (c) focusing region in the image obtained by scanning through each quarter. [12]

reflections that persist during the initial part of the reflected signals.

The imaging plane is divided into a  $20 \times 20$  grid with the dimension of  $8 \text{ mm} \times 8 \text{ mm}$  for each cell in the grid. The artifact-removed reflected signals,  $y_i(t)$  are time shifted by  $\Delta t_i$  to align the reflections arising from each grid position, where  $\Delta t_i = t_i - t_p$ ,  $t_i$  is the round-trip travel time of the signal from the  $i^{\text{th}}$  antenna position to a grid point  $(x, y)$  in the imaging plane,  $t_p = \min(t_1, t_2, t_3, \dots, t_9)$ . The time aligned reflected signals are compensated for path loss by multiplying by  $r_{i(x,y)}^4$ , where  $r_{i(x,y)}$  is the shortest electrical distance between  $i^{\text{th}}$  antenna position to the grid point  $(x, y)$ .

$$y_{i(x,y)}(t) = y_i(x,y)(t - \Delta t_i) \cdot r_{i(x,y)}^4 \quad (1)$$

In order to consider the reflections only from the grid point of interest, a 0.35 ns portion of the reflected signals,  $y_{i(x,y)}(t)$  are truncated, where 0.35 ns is the round-trip travel time of signal between two adjacent grid points inside the head. Finally, all the time-aligned and compensated signals are summed for the synthetic focusing of the reflections for that grid position. Here, signals obtained from the antenna positions which lie far apart (electrical distance  $> 12 \text{ cm}$ ) from the grid point are excluded from the synthetic focusing, to reduce clutter in the image. The maximum magnitude of the summation signal is assigned as the intensity for that grid point. The intensities of the other grid positions are calculated using similar procedure, and a 2D contour plot of the intensities of all the grid positions is represented as the reconstructed image of the head focusing on the corresponding quarter.

The imaging result for the case of one blood clot in a quarter of the head was reported earlier in [12]. The results presented here are for cases where there are multiple blood clots in any given quarter of the head model, while the imaging is done with more frequency sampling points.

The cases considered here are for the presence of either two or three blood clots of size  $1 \times 1 \times 4 \text{ cm}^3$  placed at 3 cm from the head boundary in Q1 as shown in Figure 4(a) and (b), respectively. For the case of two clots at Q1 (Figure 4a), the correct quarter shows the maximum peak intensity, however, the localization of the clots is not exact. For the case of three clots (Figure 4b), higher peak intensities are obtained at Q2 and Q3, though the clots are located at Q1. A reason for this might be the fact that the internal reflections among the clots can alter the actual signal travelling path from the anticipated path and misguide the process of signal alignment and synthetic focusing.

In both of these cases, the presence of anomaly at the correct or adjacent quarter could be suspected. However, the exact location is erroneous in these cases. The possible reasons for this could be the use of a narrow range of frequencies along with sparse frequency sampling. In addition, the high attenuation of microwave

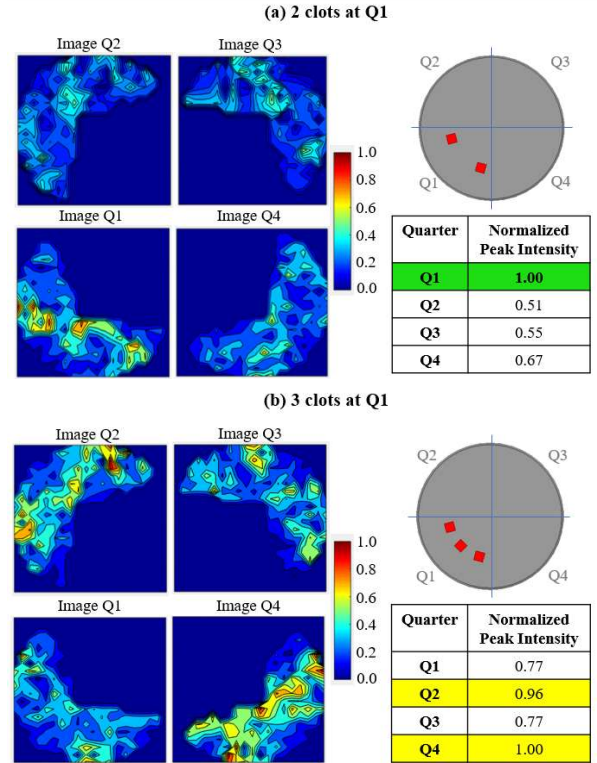


**Figure 4.** Reconstructed images for the cases of – (a) two clots in Q1, (b) three clots in Q1.

signals due to the high permittivity of brain tissue increases the ambiguity to differentiate the target reflections from clutter.

## 6. Conclusion

In this paper, the results for a microwave head imaging system incorporating a quarter-head scanning based approach utilized for the detection of blood clots inside the brain are presented. A miniaturized antipodal Vivaldi antenna is used to scan a quarter portion of a numerical head model with blood clots from nine different positions in front of each quarter in a monostatic method. The image is reconstructed from the processed reflected signals from an imaging plane, i.e., a 2D plane of the head, using a delay-and-sum beamforming method. Similarly, an image of the head is reconstructed by scanning through each of the other quarters of the head model. A comparison is made among the peak intensities of the images obtained from all four quarters, and the location of a higher intensity at any quarter indicates the possible presence and localization of anomalies, e.g., blood clots, in that quarter.

## References

- [1] J. M. Beada'a, A. M. Abbosh, D. Ireland, and M. E. Bialkowski, "Wideband antenna for microwave imaging of brain," *International Conference on Intelligent Sensors, Sensor Networks and*

- Information Processing*, December 2011, pp. 17-20, doi: 10.1109/ISSNIP.2011.6146567.
- [2] B. Mohammed, A. Abbosh, and D. Ireland, "Directive wideband antenna for microwave imaging system for brain stroke detection," *Asia Pacific Microwave Conference Proceedings*, December 2012, pp. 640-642, doi: 10.1109/APMC.2012.6421688.
- [3] B. J. Mohammed, A. M. Abbosh, and M. E. Bialkowski, "Design of tapered slot antenna operating in coupling liquid for ultrawideband microwave imaging systems," *IEEE International Symposium on Antennas and Propagation (APSURSI)*, July 2011, pp. 145-148, doi: 10.1109/APS.2011.5996662.
- [4] H. Trefna and M. Persson, "Antenna array design for brain monitoring," *IEEE Antennas and Propagation Society International Symposium*, July 2008, pp. 1-4, doi: 10.1109/APS.2008.4619683.
- [5] M. Persson *et al.*, "Microwave-based stroke diagnosis making global prehospital thrombolytic treatment possible," *IEEE Transactions on Biomedical Engineering*, **61**, 11, June 2014, pp. 2806-2817, 2014, doi: 10.1109/TBME.2014.2330554.
- [6] A. T. Mobashsher, A. Mahmoud, and A. Abbosh, "Portable wideband microwave imaging system for intracranial hemorrhage detection using improved back-projection algorithm with model of effective head permittivity," *Scientific reports*, **6**, 1, February 2016, pp. 1-16, doi: 10.1038/srep20459.
- [7] A. Abbosh, "Microwave systems for head imaging: challenges and recent developments," *IEEE MTT-S International Microwave Workshop Series on RF and Wireless Technologies for Biomedical and Healthcare Applications (IMWS-BIO)*, December 2013, pp. 1-3, doi: 10.1109/IMWS-BIO.2013.6756184.
- [8] A. T. Mobashsher, A. M. Abbosh, and Y. Wang, "Microwave system to detect traumatic brain injuries using compact unidirectional antenna and wideband transceiver with verification on realistic head phantom," *IEEE Transactions on Microwave Theory and Techniques*, **62**, 9, August 2014, pp. 1826-1836, doi: 10.1109/TMTT.2014.2342669.
- [9] S. Mustafa, B. Mohammed, and A. Abbosh, "Novel preprocessing techniques for accurate microwave imaging of human brain," *IEEE Antennas and Wireless Propagation Letters*, **12**, March 2013, pp. 460-463, doi: 10.1109/LAWP.2013.2255095.
- [10] D. Ireland and M. E. Bialkowski, "Microwave head imaging for stroke detection," *Progress In Electromagnetics Research*, **21**, October 2011, pp. 163-175, doi: 10.2528/PIERM11082907.
- [11] S. Semenov, B. Seiser, E. Stoegmann, and E. Auff, "Electromagnetic tomography for brain imaging: From virtual to human brain," *IEEE Conference on Antenna Measurements & Applications (CAMA)*, November 2014, pp. 1-4, doi: 10.1109/CAMA.2014.7003417.
- [12] F. Parveen and P. Wahid, "Microwave Head Imaging System for Detection of Blood Clots inside the Brain," *IEEE International Symposium on Antennas and Propagation and USNC-URSI Radio Science Meeting*, December 2021, © 2021 IEEE.